



Resiniferatoxin Hampers the Nocifensive Response of *Caenorhabditis elegans* to Noxious Heat, and Pathway Analysis Revealed that the Wnt Signaling Pathway is Involved

Jennifer Ben Salem^{1,2,3} · Bruno Nkambeu^{1,2} · Dina N. Arvanitis³ · Francis Beaudry^{1,2}

Received: 23 July 2021 / Revised: 13 October 2021 / Accepted: 18 October 2021 / Published online: 25 October 2021
© The Author(s), under exclusive licence to Springer Science+Business Media, LLC, part of Springer Nature 2021

Abstract

Resiniferatoxin (RTX) is a metabolite extracted from *Euphorbia resinifera*. RTX is a potent capsaicin analog with specific biological activities resulting from its agonist activity with the transient receptor potential channel vanilloid subfamily member 1 (TRPV1). RTX has been examined as a pain reliever, and more recently, investigated for its ability to desensitize cardiac sensory fibers expressing TRPV1 to improve chronic heart failure (CHF) outcomes using validated animal models. *Caenorhabditis elegans* (*C. elegans*) expresses orthologs of vanilloid receptors activated by capsaicin, producing antinociceptive effects. Thus, we used *C. elegans* to characterize the antinociceptive properties and performed proteomic profiling to uncover specific signaling networks. After exposure to RTX, wild-type (N2) and mutant *C. elegans* were placed on petri dishes divided into quadrants for heat stimulation. The thermal avoidance index was used to phenotype each tested *C. elegans* experimental group. The data revealed for the first time that RTX can hamper the nocifensive response of *C. elegans* to noxious heat (32 – 35 °C). The effect was reversed 6 h after RTX exposure. Additionally, we identified the RTX target, the *C. elegans* transient receptor potential channel OCR-3. The proteomics and pathway enrichment analysis results suggest that Wnt signaling is triggered by the agonistic effects of RTX on *C. elegans* vanilloid receptors.

Keywords *Caenorhabditis elegans* · Transient receptor potential channels · Proteomics · Mass spectrometry · Resiniferatoxin · Nociception · Wnt signaling pathway

Introduction

Resiniferatoxin (RTX) is a capsaicin analog originating from a *Euphorbia* species (*Euphorbia resinifera*) that targets the transient receptor potential channel vanilloid subfamily member 1 (TRPV1) and is several-fold more pungent than capsaicin [1]. The TRPV1 is a multisensory receptor involved in injury signaling and can be activated by various

mediators including vanilloids (e.g. capsaicin, eugenol), RTX, noxious heat (> 43 °C), acids (H⁺), and various lipids. One major pain relief strategy that has been tested in recent years includes pharmacological manipulation of TRPV1 [2–6]. However, TRPV1 activation by high doses of certain vanilloids can lead to necrosis and apoptosis [7]. RTX has been tested for chronic pain management [8] and cancer pain [9]. The activation of TRPV1 leading to an increase in the intracellular Ca²⁺ are key elements associated with the activation and sensitization of cardiac nociceptors. Thus, RTX was used to perform cardiac sympathetic afferent denervation, and the results showed that it reduces cardiac remodeling and improves cardiovascular function in a validated rat model of heart failure [10]. Chemical denervation results from the agonistic effects of RTX on TRPV1, producing an intense pungent effect and leading to cell death. Other cardiovascular benefits were observed, including a reduction in ventricular arrhythmias [11] and the lowering diastolic blood pressure [12]. Recently, we demonstrated that cardiac sensory afferent denervation by RTX during

✉ Francis Beaudry
francis.beaudry@umontreal.ca

¹ Groupe de Recherche en Pharmacologie Animal du Québec (GREPAQ), Département de Biomédecine Vétérinaire, Faculté de Médecine Vétérinaire, Université de Montréal, Saint-Hyacinthe, Québec, Canada

² Centre de recherche sur le cerveau et l'apprentissage (CIRCA), Université de Montréal, Montréal, Québec, Canada

³ Institut des Maladies Métaboliques et Cardiovasculaires, INSERM UMR1297, Université de Toulouse, Toulouse, France

myocardial infarction could modulate long-term susceptibility to anxiodepressive behavior using a validated mouse model of chronic heart failure [13]. Treatment with RTX triggered the desensitization of cardiac afferents and hampered the anxiodepressive-like state in mice. Depression and anxiety are widely observed in patients suffering chronic heart failure [14]. Additionally, we found unique protein profiles and regulatory pathways in the frontal cortices that are associated with the response to stresses originating from the heart [13]. RTX treatment produces unique brain signaling patterns that require further characterization. To extend our knowledge, we intend to use a model organism for which a large proportion of its genes have functional counterparts in mammals, which therefore makes these models exceptionally useful to study biological processes and diseases in mammals, including humans [15].

Caenorhabditis elegans (*C. elegans*) is a very interesting model organism, particularly in the context of functional genomics relevant to mammalian and human biology and diseases [15–17]. *C. elegans* genome sequencing was completed in 1998 and is publicly available and well annotated. This is a significant benefit of proteomics, as it enables the interpretation of functionally grouped gene ontology (GO) and pathway annotation networks [18]. There are roughly ~21,000 predicted protein-coding genes in *C. elegans*. Notably, many of these genes are shared with mammals, including humans [19, 20]. *C. elegans* adults consist of 959 cells, of which 302 are neurons, making this model a valuable model organism to study the nervous system [21]. Thus, *C. elegans* is particularly useful to study nociception, as the animal displays well-defined and reproducible nocifensive behavior involving a reversal and change in direction away from noxious stimuli. In mammals, important molecular transducers of noxious stimuli include ligand-gated (e.g. TRPV1, TRPA1) and voltage-gated (Nav1.7, Nav1.8, Nav1.9) ion channels [22]. Following *C. elegans* genome sequencing, several genes encoding TRP ion channels with important sequence homologies to mammalian TRP channels, including TRPVs, were identified [23]. More specifically, five TRPV orthologs (e.g., OSM-9, OCR-1, OCR-2, OCR-3 and OCR-4) were discovered and studied [24]. Furthermore, several studies have shown that *C. elegans* TRPV orthologs are associated with behavioral and physiological processes, including sensory transduction [2, 3, 25, 26]. Additionally, it was determined that *C. elegans* TRPV channels share similar activation and regulatory mechanisms with higher species, including mammals. Interestingly, our recent paper revealed that capsaicin can impede the nocifensive response of *C. elegans* to noxious heat (i.e. 32–35 °C) following sustained exposure, and this effect was reversed 6 h after capsaicin exposure [2]. Furthermore, data suggest that capsaicin targets the *C. elegans* transient receptor potential ion channel OCR-2. Additional experiments

indicated that other capsaicin analogs have antinociceptive effects, including olvanil, gingerol, shogaol and curcumin, as well as for other vanilloids, including eugenol, vanillin and zingerone [3]. Thus, known TRPV ligands that target *C. elegans* vanilloid receptors and produce antinociceptive effects compatible with previous studies were performed using animal models of pain.

Our hypothesis is that RTX will interact with TRPV ortholog channels in *C. elegans* in a manner similar to that of capsaicin, and sustained exposure to RTX will hamper the nocifensive response of *C. elegans* to noxious heat. The objective of this study was to (1) characterize the RTX exposure–response relationships using *C. elegans* and heat avoidance behavior analysis [27] and (2) perform proteomics to identify the proteins and pathways responsible for the induced phenotype.

Materials and Methods

Chemicals and Reagents

All chemicals and reagents were obtained from Fisher Scientific (Fair Lawn, NJ, USA) or Millipore Sigma (St. Louis, MO, USA). Capsaicin was purchased from Toronto Research Chemicals (North York, ON, CAN). RTX was obtained from Tocris Bioscience (Rennes, France).

Caenorhabditis elegans Strains

The N2 (Bristol) isolate of *C. elegans* was used as a reference strain. The mutant strains used in this study included *ocr-1* (ak46), *ocr-2* (yz5), *ocr-3* (ok1559), *ocr-4* (vs137) and *osm-9* (yz6). N2 (Bristol) and other strains were obtained from the *Caenorhabditis* Genetics Center (CGC), University of Minnesota (Minneapolis, MN, USA). Strains were maintained and manipulated under standard conditions as previously described [28, 29]. Nematodes were grown and kept on nematode growth medium (NGM) agar at 22 °C in a Thermo Scientific Heratherm refrigerated incubator (Fair Lawn, NJ, USA). Analyses were executed at room temperature (~ 22 °C) unless otherwise noted.

Caenorhabditis elegans Pharmacological Manipulations

Capsaicin or RTX was dissolved in Type 1 Ultrapure Water at a concentration of 25 µM. The solutions were warmed for brief periods combined with vortexing and sonication for several minutes to completely dissolve the compounds. Further dilutions to concentrations of 5 µM, 1 µM and 0.1 µM in Type 1 Ultrapure Water were performed by serial dilution of the RTX stock solution. *C. elegans* was isolated

and washed according to the protocol outlined by Margie et al. [29]. After 72 h of feeding and growing on 92 × 16 mm petri dishes with NGM, the nematodes were denied food and exposed to capsaicin or RTX solutions. An aliquot of 7 mL of a capsaicin or RTX solution was added to produce a 2–3 mm solution film (the solution was partly absorbed by NGM); consequently, the nematodes swam in solution. *C. elegans* was exposed to capsaicin or RTX for 60 min and isolated and washed thoroughly prior to the behavioral experiments. For the residual effect (i.e. 6 h latency) evaluation, after exposure to the RTX solutions, the nematodes were isolated, carefully washed and deposited on NGM free of RTX for 6 h prior to testing.

Thermal Avoidance Assays

The method we proposed in this manuscript for the evaluation of thermal avoidance was modified from the four quadrant strategy previously described [27] and used in previous successfully published work [2, 3]. Briefly, experiments were performed on 92 × 16 mm petri dishes divided into four quadrants. A middle circle delimited (i.e. 1 cm diameter) an area where *C. elegans* were not considered. Petri dishes were divided into quadrants: two stimulus areas (A and D) and two control areas (B and C). Sodium azide (0.5 M) was used in all quadrants to paralyze the nematodes. Noxious heat was created with an electronically heated metal tip (0.8 mm in diameter) producing a radial temperature gradient (e.g., 32–35 °C on NGM agar 2 mm from the tip measured with an infrared thermometer). Nematodes were isolated and washed according to a protocol outlined by Margie et al. [29]. The nematodes tested were denied food during all experimentations. The nematodes (typically 100–1000 young adult nematodes) were placed at the center of a marked petri dish, and after 30 min, the plates were placed at 4 °C for at least 1 h, and the number of nematodes per quadrant were counted. Nematodes that did not cross the inner circle were not considered. The thermal avoidance index (TI) was calculated as shown in Eq. 1.

$$TI = \frac{[(A + D) - (B + C)]}{(A + B + C + D)}$$

Details are shown in supplementary Figure S1. Both the TI and the animal avoidance percentage were used to phenotype each tested *C. elegans* experimental group. The stimulus temperature used was based on previous experiments [30].

Proteomic Analysis

Cultured nematodes (with or without RTX exposure) were collected in liquid media and centrifuged at 1000 g

for 10 min; the nematodes were then collected and thoroughly washed. Nematodes were resuspended in 8 M urea in 100 mM TRIS-HCl buffer (pH 8) containing cComplete™ protease inhibitor cocktails (Roche Diagnostic Canada, Laval, QC, Canada) and aliquoted into reinforced 1.5 mL homogenizer tubes containing 500 µm glass bead homogenizer tubes with 25 mg of glass beads. The samples were homogenized using a Bead Mill Homogenizer (Fisher) with 3 bursts of 60 s at a speed of 5 m/s. The homogenates were centrifuged at 9000 g for 10 min. The protein concentration for each homogenate was determined using a Bradford assay. Two hundred micrograms of protein was extracted using ice-cold acetone precipitation (1:5, v/v). The protein pellet was dissolved in 100 µL of 50 mM TRIS-HCl buffer (pH 8), and the solution was mixed with a Disruptor Genie at maximum speed (2800 rpm) for 15 min and sonicated to improve the protein dissolution yield. The proteins were denatured by heating at 120 °C for 10 min using a heated reaction block. The solution was allowed to cool 15 min. Proteins were reduced with 20 mM dithiothreitol (DTT), and the reaction was performed at 90 °C for 15 min. Then, proteins were alkylated with 40 mM iodoacetamide (IAA) protected from light at room temperature for 30 min. Then, 5 µg of proteomic-grade trypsin was added, and the reaction was performed at 37 °C for 24 h. Protein digestion was quenched by adding 10 µL of a 1 % trifluoroacetic acid (TFA) solution. Samples were centrifuged at 12,000 g for 10 min, and 100 µL of the supernatant was transferred into injection vials for analysis. The HPLC system was a Thermo Scientific Vanquish FLEX UHPLC system (San Jose, CA, USA). Chromatography was performed using gradient elution along with a Thermo Biobasic C18 microbore column (150 × 1 mm) with a particle size of 5 µm. The initial mobile phase conditions consisted of acetonitrile and water (both fortified with 0.1 % formic acid) at a ratio of 5:95. From 0 to 3 min, the ratio was maintained at 5:95. From 3 to 123 min, a linear gradient was applied up to a ratio of 40:60, which was maintained for 3 min. The mobile phase composition ratio was the reverted to the initial conditions, and the column was allowed to re-equilibrate for 30 min. The flow rate was fixed at 50 µL/min, and 5 µL of each sample was injected. A Thermo Scientific Q Exactive Plus Orbitrap Mass Spectrometer (San Jose, CA, USA) was interfaced with the UHPLC system using a pneumatic-assisted heated electrospray ion source. Nitrogen was used as the sheath and auxiliary gases, which were set at 15 and 5 arbitrary units, respectively. The auxiliary gas was heated to 200 °C. The heated ESI probe was set to 4000 V, and the ion transfer tube temperature was set to 300 °C. Mass spectrometry (MS) detection was performed in positive ion mode operating in TOP-10 data dependent acquisition (DDA) mode. A DDA cycle entailed one MS¹ survey scan (m/z 400–1500) acquired at 70,000 resolution (FWHM) and precursor ions meeting

the user-defined criteria for charge state (i.e. $z = 2, 3$ or 4), monoisotopic precursor intensity (dynamic acquisition of MS^2 -based TOP-10 most intense ions with a minimum 1×10^4 intensity threshold). Precursor ions were isolated using the quadrupole (1.5 Da isolation width), activated by HCD (28 NCE) and fragment ions were detected in the ORBITRAP at a resolution of 17,500 (FWHM). Data were processed using Thermo Proteome Discoverer (version 2.4) in conjunction with SEQUEST using default settings unless otherwise specified. The identification of peptides and proteins with SEQUEST was performed based on the reference proteome extracted from UniProt (*C. elegans* taxon identifier 6239) as FASTA sequences. Parameters were set as follows: MS^1 tolerance of 10 ppm; MS^2 mass tolerance of 0.02 Da for Orbitrap detection; enzyme specificity was set as trypsin with two missed cleavages allowed; carbamidomethylation of cysteine was set as a fixed modification; and oxidation of methionine was set as a variable modification. The minimum peptide length was set to six amino acids. Data sets were further analyzed with Percolator. Peptide-spectrum matches (PSMs) and protein identification were filtered at a 1% false discovery rate (FDR) threshold. For protein quantification and comparative analysis, we used the peak integration feature of Proteome Discoverer 2.4 software. For each identified protein, the average ion intensity of the unique peptides was used for protein abundance.

Bioinformatics

Abundance Ratio (\log_2): (experimental group)/(N2 control), Abundance Ratio P-Value: (experimental group)/(N2 control) and Accession columns were extracted from the data sets generated by Proteome Discoverer. Volcano plots were generated using all identified and quantified proteins with both a \log_2 ratio and p-value. Proteins without a p-value or with a p-value > 0.01 were not used for further functional analysis. Additionally, only proteins with an absolute \log_2 ratio ≥ 1.0 were used for bioinformatics analysis. Gene Ontology analysis of genes (i.e. GO terms) was performed using Metascape [31], where two sets of proteins (e.g. Ensembl gene codes) were used: proteins with a \log_2 ratio ≥ 1.0 (i.e. upregulated) and proteins with a \log_2 ratio ≤ -1.0 (downregulated). The results from the upregulated and downregulated protein analyses were used to create bar plots in PRISM using the Metascape reports with the $-\log_{10}$ p-value of GO process matches given by Metascape. Further pathway analysis was performed using ClueGO [32] and Cytoscape [33] using the KEGG and REACTOME pathway databases. Significant pathways for proteins with an absolute \log_2 ratio ≥ 1.0 were identified, comparing the ratio of target genes identified in each pathway to the total number of genes within the pathway. The statistical test used to determine the enrichment score for KEGG or REACTOME pathways

was based on a right-sided hypergeometric distribution with multiple testing correction (Benjamini & Hochberg (BH) method) [34].

Statistical Analysis

Behavioral data were analyzed using one-way ANOVA followed by Dunnett's multiple comparison test (e.g. WT (N2) was the control group) or ANOVA followed by a Tukey-Kramer multiple comparison test. Data presented in Fig. 1 were analyzed using ANOVA followed by Sidak's multiple comparisons test for specific pairwise comparisons. Significance was set a priori to $p < 0.05$. Statistical analyses were performed using PRISM (version 9.1.2).

Results and Discussion

Recently, we demonstrated for the first time the antinociceptive effects of capsaicin in *C. elegans* following controlled and prolonged exposure [2]. Further analysis revealed that capsaicin targets OCR-2, one of the five vanilloid receptor orthologs (e.g., OSM-9, OCR-1, OCR-2, OCR-3 and OCR-4). Moreover, we have shown that other vanilloids, including eugenol, induce similar antinociceptive effects [3]. The thermal avoidance assay performed is described in supplementary Figure S1 and was specifically used to assess the antinociceptive effects of RTX. The first step was to verify whether there was bias in *C. elegans* behavior using the experimental setup. Thus, we performed an assessment of the mobility and bias of WT (N2) nematodes with and without exposure to RTX. As shown in Fig. 1, no quadrant selection bias was observed for all *C. elegans* experimental groups tested with or without RTX exposure (e.g., 5, 1 and $0.1 \mu\text{M}$). The data demonstrated that the nematodes did not select any specific quadrant and were uniformly distributed 30 min after the initial nematode deposition at the center of the petri dish. Sixty minutes of RTX exposure did not appear to affect nematode mobility. In a previous study, we tested mutant nematodes *ocr-1*, *ocr-2*, *ocr-3*, *ocr-4* and *osm-9* [2, 3], and no bias was observed.

Prolonged stimulation with TRPV1 agonists elicits receptor desensitization, leading to the alleviation of pain (or antinociceptive effects in *C. elegans*) [4]. Consequently, we exposed *C. elegans* to RTX in solution for the complete control of time and exposure levels. As presented in Fig. 2, the data revealed antinociceptive effects following a 1 h of exposure, which were, to a certain extent concentration-dependent. The antinociceptive effects of RTX were noted even at a very low concentration ($0.1 \mu\text{M}$), and RTX was found to be significantly more potent than capsaicin [2]. These observations are consistent with previously published *in vitro* and *in vivo* testing data [35, 36]. Following

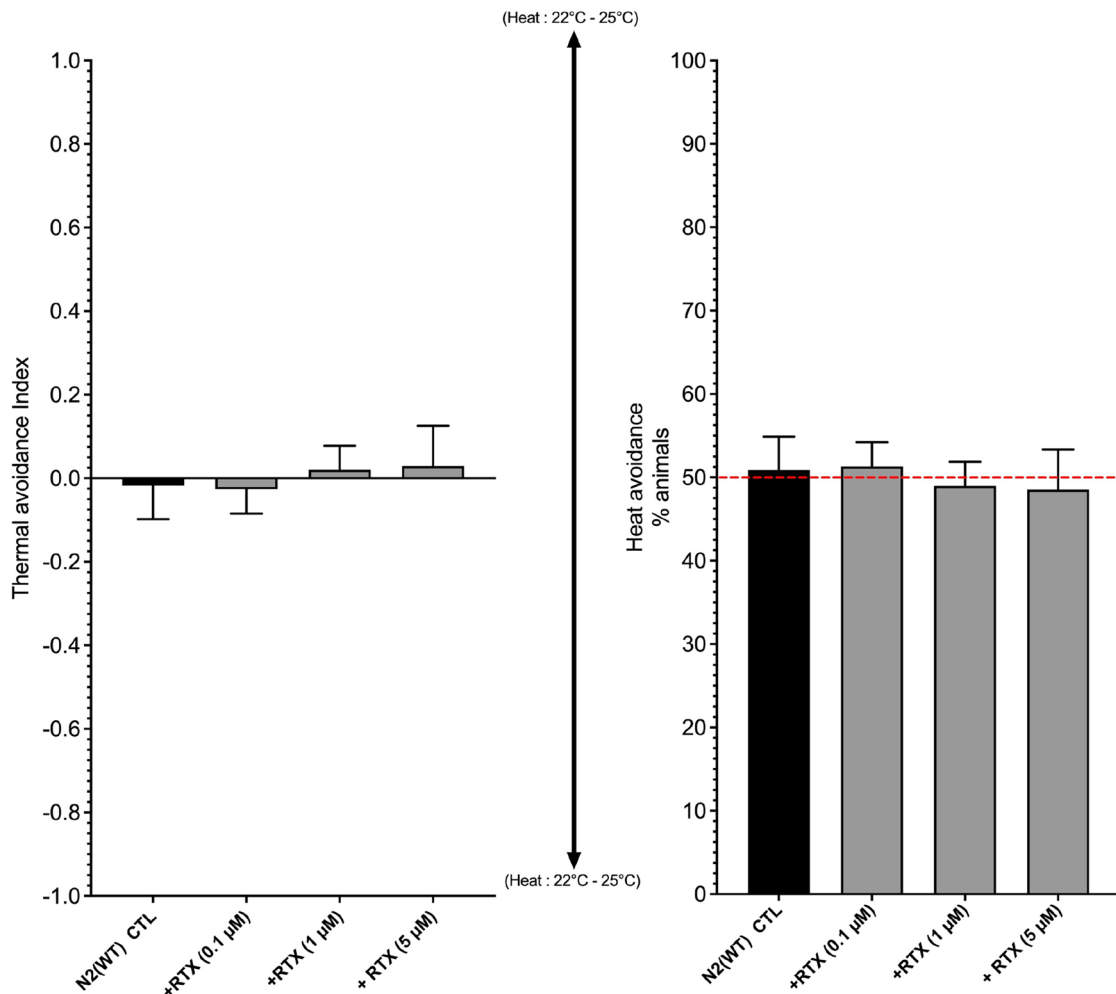


Fig. 1 Comparison of the mobility and bias of WT (N2) nematodes in plates divided into quadrants conserved at a constant temperature (22 °C) without the application of a stimulus (negative control). Display values (means \pm SD) were calculated from at least 6 independ-

ent experiments for each experimental group. No quadrant selection bias was observed for any *C. elegans* genotype tested in the absence or presence of RTX at 5 μ M, 1 μ M and 0.1 μ M

RTX exposure, the nematodes were carefully washed and transferred to NGM agar maintained at 22 °C in an incubator for 6 h (i.e., residual effect/latency test). Then, the thermal avoidance response was retested. As shown in Fig. 2, the results indicated that 6 h after exposure to RTX, the *C. elegans* thermal avoidance response returned to normal, confirming that no residual antinociceptive effects of RTX were observed after 6 h. These results were unexpected and are quite interesting since RTX is apoptotic [7, 8, 37] and the local application of RTX has been used for chemical denervation [13, 38]. The results suggest that RTX does not induce a long-lasting effect. Additionally, the results indicate that RTX does not induce significant damage to the sensory system at a concentration \leq 5 μ M and a 60-min exposure period.

The target of RTX needs to be identified to better understand the exposure–response relationship. Pharmacological

effects can be measured when the tested molecule binds to a sufficient fraction of the target receptor, leading to a specific response (i.e., physiological or phenotypic changes). Accordingly, we conducted experiments using specific *C. elegans* mutants (*ocr-1*, *ocr-2*, *ocr-3*, *ocr-4* and *osm-9*) to potentially identify the RTX target receptors. As revealed in Fig. 3, all mutants appeared less sensitive to noxious heat than the WT (N2) group. However, they were still sensitive, which suggests redundancy in receptor function. These results are compatible with our previous findings [2, 3]. To identify targets, we used the concentration at which RTX maximum response was achieved, specifically 1 μ M as display in Fig. 2. Thus, *C. elegans* mutants were exposed to RTX at a concentration of 1 μ M for 60 min prior to the behavioral experiments. Figure 3 shows that the RTX antinociceptive effects were quantifiable in the *ocr-1*, *ocr-2*, *ocr-4* and *osm-9* mutants. However, no significant RTX effects (p

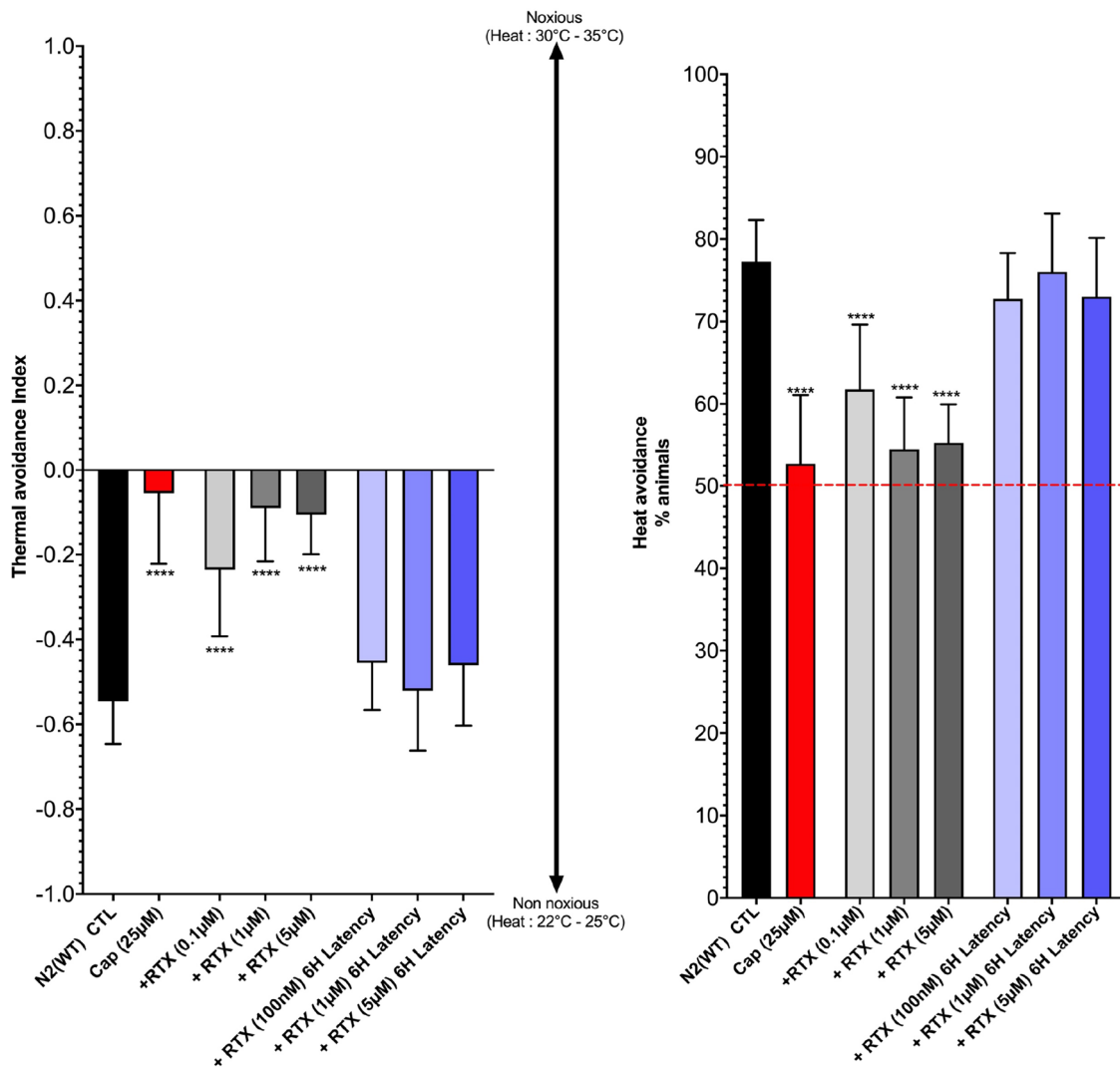


Fig. 2 Assessment of the pharmacological effects of RTX on thermal avoidance in *C. elegans*. Nematodes were exposed to RTX or capsaicin (Cap) for 60 min prior to behavior experimentation. Display values (means ± SD) were calculated from at least 12 independent experiments for each experimental group. The observed effects of RTX are dose-dependent and noticeably hamper thermal avoidance in

C. elegans. **** $p < 0.0001$ (ANOVA - Tukey-Kramer multiple comparison test). The results suggest an effect similar to that of capsaicin but at a notably lower concentration. No residual antinociceptive effects were observed 6 h after exposure (ANOVA - Dunnett’s multiple comparison versus CTL group). Additional Cap data can be found in Nkambeu et al. 2020 [2]

> 0.05) were observed with the *ocr-3* mutant, suggesting that RTX targets OCR-3, a mammalian vanilloid receptor-like channel. Some interactions between RTX and other vanilloid receptors may happen, most likely with lower specificity. These results were unexpected since our previous results clearly showed that capsaicin targets the OCR-2 receptor, not OCR-3 [2]. Additionally, we showed that other vanilloids target OCR-2 [3]. As shown by another study, heat avoidance is mediated by OSM-9 and OCR-2 in *C. elegans* [25]. The functions of OCR-3 are unknown, but it is coexpressed with OSM-9 [39]. There is no clear evidence that OCR-3 is activated by nociceptive heat, but it is predicted to enable ion channel activity and is classified as capsaicin

receptor-related. Little is known about this vanilloid receptor, and further study is required to elucidate OCR-3 function in *C. elegans*.

Label-free proteomic investigations were performed on *C. elegans* exposed to 1 µM RTX for 60 min. Figure 4 shows volcano plots illustrating the differential abundances of proteins, with the x-axis representing the \log_2 ratio and the y-axis plotting $-\log_{10}$ (P-value). The colored boxes represent a 2-fold change and $p\text{-value} \leq 0.05$. Several differentially expressed proteins (DEPs) were identified, including 157 upregulated and 305 downregulated proteins. Moreover, we extracted specific data related to vanilloid receptor proteins (i.e., OCR-1, OCR-2, OCR-3, OCR-4 and OSM-9) and the

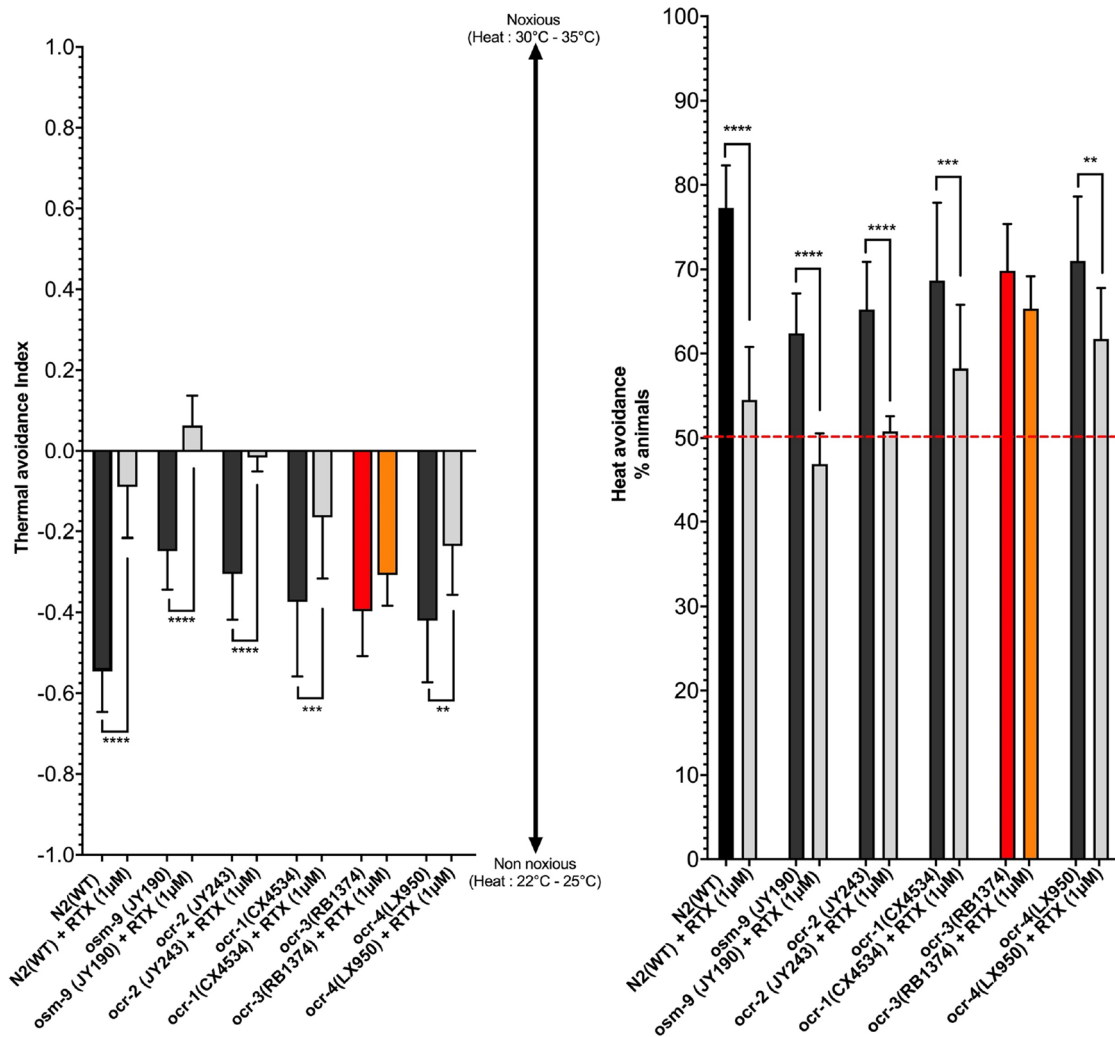


Fig. 3 Identification of TRPV orthologs responsible for the RTX-induced antinociceptive effects. Display values (means \pm SD) were calculated from at least 12 independent experiments for each experimental group. The data strongly suggest that RTX exerts antinociceptive

effects through the ORC-3 *C. elegans* TRPV ortholog. **** $p < 0.0001$, *** $p < 0.001$, ** $p < 0.01$ (ANOVA - Sidak's multiple comparisons test using specific comparison pairs)

NPR-1 signaling pathway [25, 27]. Interestingly, OCR-1, OCR-2, OCR-3, OCR-4, OSM-9, FLP-18 and FLP-21 were significantly upregulated. Both FLP-18 and FLP-21 are important neuropeptides that interact with NPR-1 and are involved in heat sensory processes [25, 27]. Vanilloid receptors are mainly heat thermosensors and calcium-selective channels. Upregulation of vanilloid receptors can increase neuron depolarization, leading to receptor desensitization and conformational changes. These are major mechanisms that lead to the alleviation of pain or antinociceptive effects in *C. elegans*.

Gene Ontology (GO) term enrichment analysis was performed using Metascape [31], and label-free proteomic results included all differentially expressed proteins (DEPs). The top enriched terms are shown in Fig. 5A. GO annotation indicated that the differentially expressed

proteins were mainly enriched in cellular energy processes, cellular component organization, biosynthesis of amino acids and peptide synthesis and metabolic processes. Moreover, cellular homeostasis is a process associated with ion homeostasis (Ca^{2+} , K^{+} , Cl^{-} and others). This process is essential to maintain a steady state at the cellular level. RTX is a pungent TRPV1 ligand and activates inward currents due to calcium influx, resulting in cell depolarization. Calcium ion accumulation can provoke apoptosis, and this is the mechanism at the heart of chemical denervation using the agonistic effects of RTX on TRPV1 [10, 13]. Interestingly, apoptosis or cell death terms were not among the top enriched GO terms. This is certainly compatible with the behavior results showing that the nematodes completely recovered noxious heat sensitivity at 6 h after RTX exposure, as shown

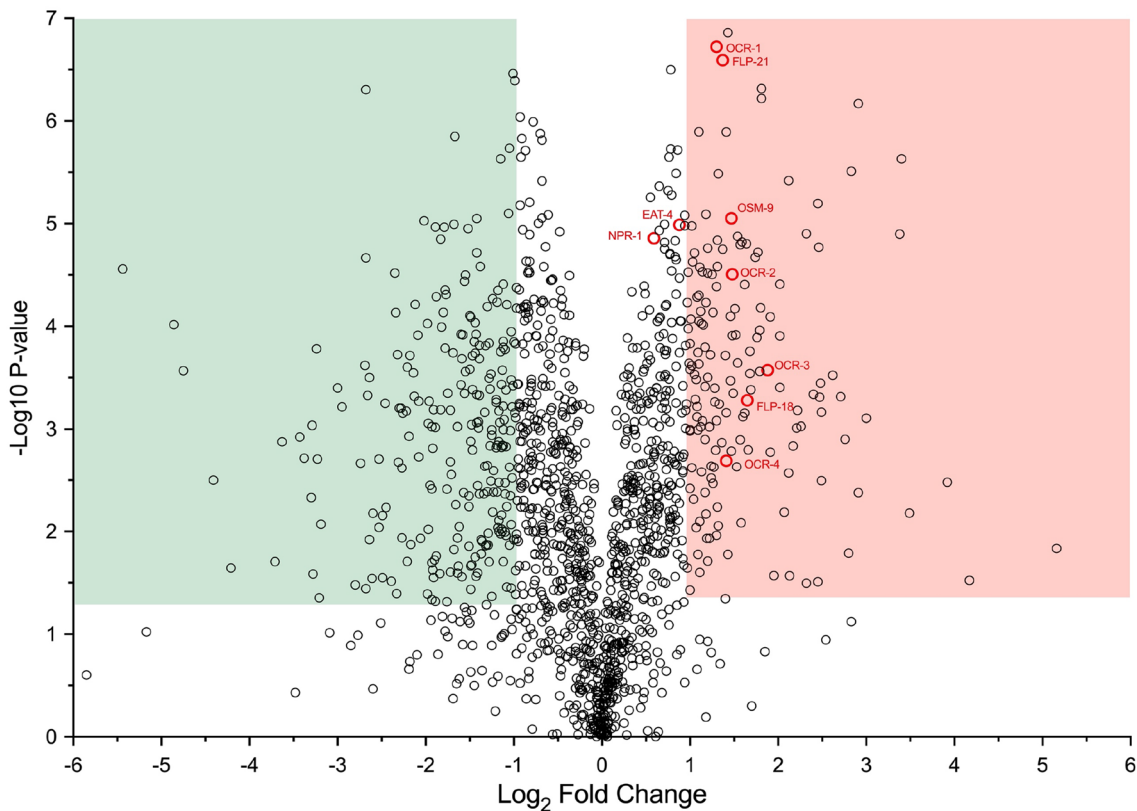


Fig. 4 Volcano plot illustrating differential abundances of proteins with the x-axis showing the log₂ ratio with respect to the control (N2) and the y-axis representing the $-\log_{10}$ of the p-value. Boxes illustrate a p-value of 0.05, and the positions of the 1.0 and -1.0 log₂ ratios that correspond to twofold increases/decreases are colored

green and red, respectively. A total of 157 upregulated and 305 downregulated proteins were observed. Interestingly, vanilloid receptor proteins (OCR1-4 and OSM-9) and specific proneuropeptides (FLP-21 and FLP-18) were significantly upregulated following 60 min of exposure to RTX

in Fig. 2. Consequently, RTX did not provoke nociceptive neuronal death. Kyoto Encyclopedia of Genes and Genomes (KEGG) and REACTOME pathway analyses were performed using ClueGO including all DEPs [32]. The top pathway enrichments are revealed in Fig. 5B. As expected, the results were compatible with the GO term enrichment results, with an important emphasis on cellular energy processes and metabolism. ClueGO identified all statistically enriched pathways, and cumulative hypergeometric p-values and enrichment factors were calculated and used for filtering. Selected significant pathways were clustered hierarchically into an interactome created based on Kappa-statistical similarities among their genes (i.e., encoding protein) memberships. Subsequently, a kappa score of 0.8 was applied as the threshold to produce interactome and pathway clusters. The network analysis and interaction between the enriched KEGG and REACTOME pathways are shown in Fig. 6. Interestingly, we observed an interaction between the cellular response to chemical stress, beta-catenin-independent Wnt signaling and ion homeostasis. This clearly suggests that these processes

are associated with the pungent effects of RTX on the *C. elegans* vanilloid receptor, most likely OCR-3, as shown in Fig. 3. The interaction with metabolic processes seems to suggest that they will trigger cellular energy processes involved in catabolism and anabolism reactions. Severe metabolic stress can lead to a state of cell survival, and notably, energy metabolism processes can rescue the cell from apoptosis. However, we were particularly interested in the beta-catenin-independent Wnt signaling pathway. Wnt signaling activates several different intracellular pathways essential to cell proliferation, differentiation, and polarity [40]. Moreover, in *C. elegans*, the Wnt signaling pathway regulates the subcellular positioning of presynaptic terminals and is therefore important for the assembly of synapses, a key component in the formation of neural circuits [41]. Dysfunction in key Wnt pathway components can lead to disorders including depression and anxiety [40, 42, 43]. This is consistent with our observation that RTX denervation of cardiac sensory afferents led to a significant reduction in depressive behavior in a mouse model of chronic heart failure [13]. During this study,

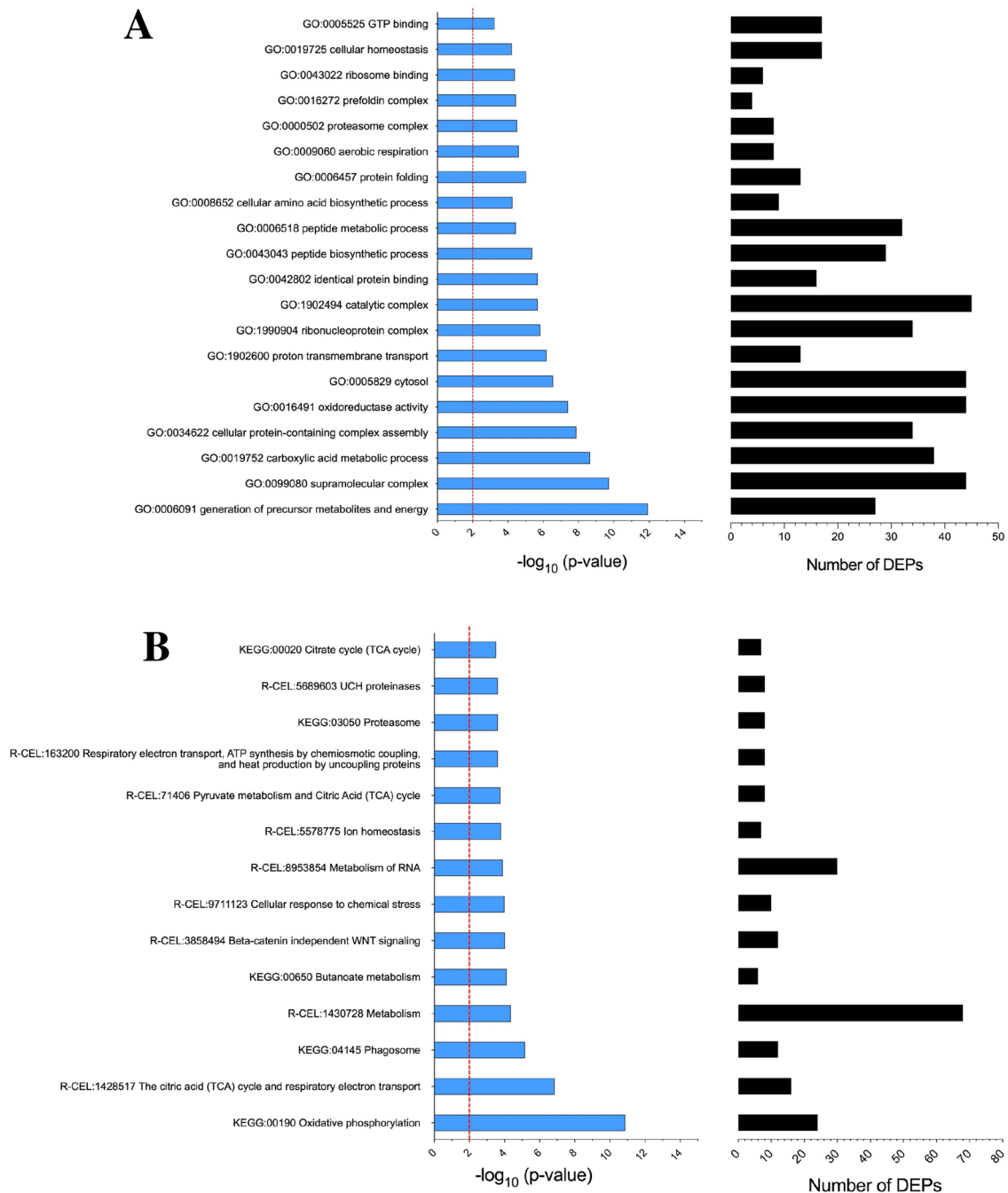


Fig. 5 Gene ontology (GO), Kyoto Encyclopedia of Genes and Genomes (KEGG) and REACTOME enriched terms. Analysis was performed with all DEPs (upregulated and downregulated). (A) Detailed information relating to changes in the biological processes

(BPs), cellular components (CCs), and molecular functions (MFs) of the DEPs following RTX exposure through GO enrichment analyses. (B) KEGG and REACTOME pathway enrichment analysis

we also demonstrated the importance of the Wnt signaling pathway. The noncanonical beta-catenin-independent Wnt pathway is linked with Ca^{2+} release from intracellular stores, and an increase in intracellular Ca^{2+} concentration can activate the mitogen-activated protein kinase (MAPK)

pathway. Subsequently, this pathway will negatively regulate the canonical Wnt pathway by inhibiting gene transcription mediated by the beta-catenin/TCF complex [42]. Interestingly, canonical Wnt pathway antagonists can effectively mediate depressive behavior [42, 43].

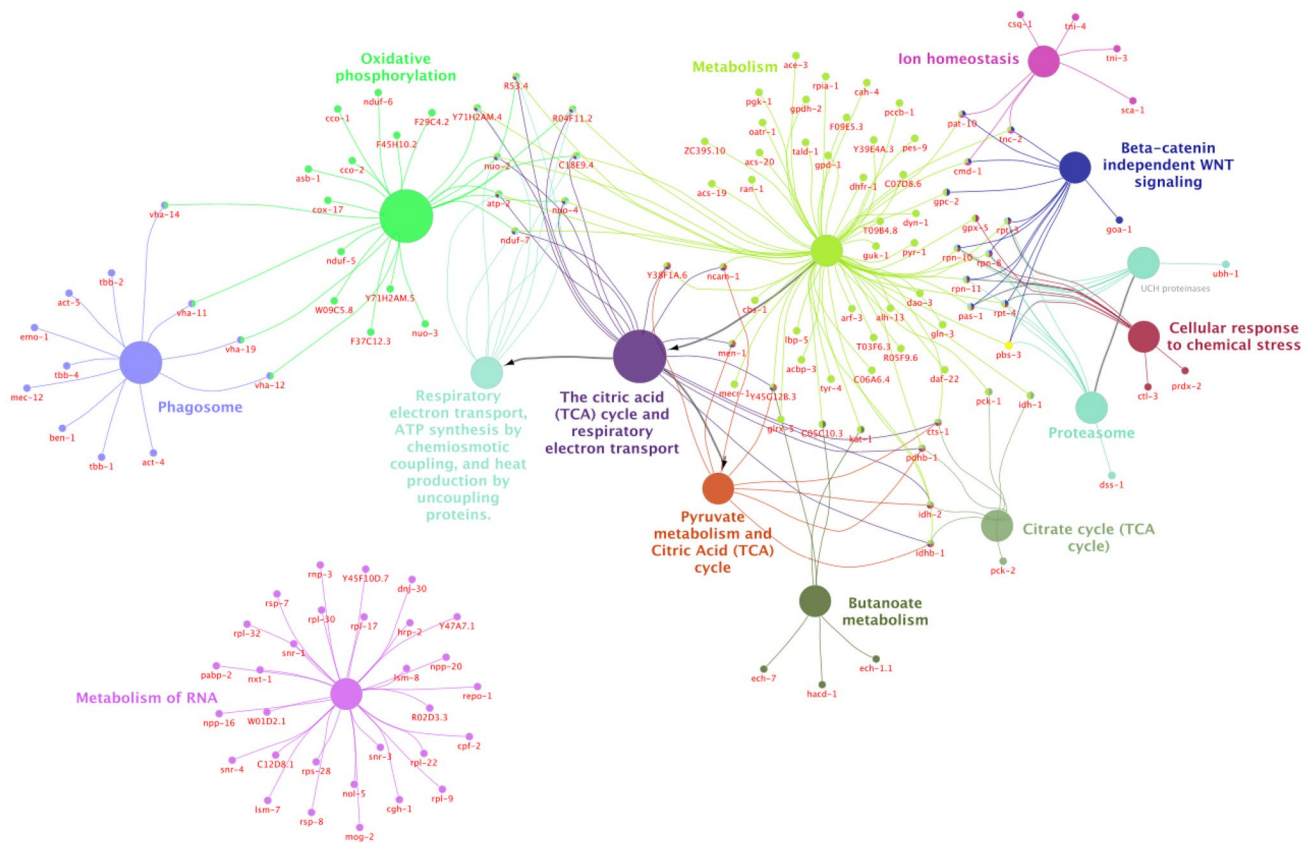


Fig. 6 Network analysis and interactions between the enriched KEGG and REACTOME pathways. The network is colored by cluster ID. Please note that nodes sharing the same cluster ID are commonly close to each other. We applied a 0.8 kappa score as the threshold

Conclusions

This study has shown for the first time the antinociceptive effects of RTX in *C. elegans* following controlled and prolonged exposure. Moreover, our results suggest that RTX targets the *C. elegans* vanilloid receptor ortholog OCR-3 and not OCR-2, which is the target of capsaicin. Proteomics and bioinformatics analyses revealed that the effects observed with RTX might be related to the noncanonical beta-catenin-independent Wnt pathway leading to negative regulation of the canonical Wnt pathway. This discovery is consistent with our previous study, where we showed that RTX denervation of cardiac sensory afferents yielded a significant reduction in depressive-like behavior in a mouse model of chronic heart failure [7].

Supplementary Information The online version contains supplementary material available at <https://doi.org/10.1007/s11064-021-03471-2>.

Acknowledgements This project was funded by the National Sciences and Engineering Research Council of Canada (F. Beaudry discovery Grant Nos. RGPIN-2015-05071 and RGPIN-2020-05228). Laboratory equipment was funded by the Canadian Foundation for Innovation (CFI) and the *Fonds de Recherche du Québec (FRQ)*, the Government

of Quebec (F. Beaudry CFI John R. Evans Leaders Grant No. 36706). Ph.D. scholarships were awarded to J. Ben Salem from the Fonds de Recherche du Québec - Santé and from the Université de Montréal.

Data Availability Data generated or analyzed during this study are included in the supplementary material.

Declarations

Conflict of interest The authors declare they have no conflicts of interest.

References

1. Carnevale V, Rohacs T (2016) TRPV1: A target for rational drug design. *Pharmaceuticals (Basel)* 9(3):52
2. Nkambeu B, Ben Salem J, Beaudry F (2020) Capsaicin and its analogues impede nocifensive response of caenorhabditis elegans to noxious heat. *Neurochem Res* 45:1851–1859
3. Nkambeu B, Ben Salem J, Beaudry F (2021) Eugenol and other vanilloids hamper Caenorhabditis elegans response to noxious heat. *Neurochem Res* 46(2):252–264
4. Jara-Oseguera A, Simon SA, Rosenbaum T (2008) TRPV1: on the road to pain relief. *Curr Mol Pharmacol* 1(3):255–269

5. Guénette SA, Ross A, Marier J-F, Beaudry F (2007) Pharmacokinetics of eugenol and its effects on thermal hypersensitivity in rats. *Euro J Pharmacol* 562:60–67
6. Beaudry F, Ross A, Lema PP, Vachon P (2010) Pharmacokinetics of vanillin and its effects on mechanical hypersensitivity in a rat model of neuropathic pain. *Phytother Res* 24:525–530
7. Ramírez-Barrantes R, Córdova C, Gatica S, Rodríguez B, Lozano C, Marchant I, Echeverría C, Simon F, Olivero P (2018) Transient receptor potential vanilloid 1 expression mediates capsaicin-induced cell death. *Front Physiol* 9:682
8. Brown DC, Resiniferatoxin (2016) The evolution of the “Molecular Scalpel” for chronic pain relief. *Pharmaceuticals (Basel)* 9(3):47
9. de Almeida AS, Bernardes LB, Trevisan G (2021) TRP channels in cancer pain. *Eur J Pharmacol* 904:174185
10. Wang HJ, Wang W, Cornish KG, Rozanski GJ, Zucker IH (2014) Cardiac sympathetic afferent denervation attenuates cardiac remodeling and improves cardiovascular dysfunction in rats with heart failure. *Hypertension* 64(4):745–755
11. Wu Y, Hu Z, Wang D, Lv K, Hu N (2020) Resiniferatoxin reduces ventricular arrhythmias in heart failure via selectively blunting cardiac sympathetic afferent projection into spinal cord in rats. *Eur J Pharmacol* 15:172836
12. Wang HJ, Rozanski GJ, Zucker IH (2017) Cardiac sympathetic afferent reflex control of cardiac function in normal and chronic heart failure states. *J Physiol* 595(8):2519–2534
13. Kermorgant M, Ben Salem J, Iacovoni JS, Calise D, Dahan L, Guiard BP, Lopez S, Lairez O, Lasbories A, Nasr N, Pavy Le-Traon A, Beaudry F, Senard JM, Arvanitis DN (2021) Cardiac sensory afferents modulate susceptibility to anxio-depressive behaviour in a mouse model of chronic heart failure. *Acta Physiol (Oxf)* 231(4):e13601
14. Bordoni B, Marelli F, Morabito B, Sacconi B (2018) Depression and anxiety in patients with chronic heart failure. *Future Cardiol* 14(2):115–119
15. Apfeld J, Alper S (2018) What can we learn about human disease from the Nematode *C. elegans*. *Methods Mol Biol* 1706:53–75
16. Komuniecki R et al (2012) Monoamines activate neuropeptide signaling cascades to modulate nociception in *C. elegans*: a useful model for the modulation of chronic pain? *Invertebr Neurosci* 12:53–61
17. Avila D et al (2012) The *Caenorhabditis elegans* model as a reliable tool in neurotoxicology. *Human Exp Toxicol* 31(3):236–243
18. Cao R et al. Quantitative Proteomic Analysis of Membrane Proteins Involved in Astroglial Differentiation of Neural Stem Cells by SILAC Labeling Coupled with LC–MS/MS. *Journal of Proteome Research*. 2012;11:829–838
19. Kim Y, Park Y, Hwang J, Kwack K (2018) Comparative genomic analysis of the human and nematode *Caenorhabditis elegans* uncovers potential reproductive genes and disease associations in humans. *Physiol Genomics* 50(11):1002–1014
20. Kim W, Underwood RS, Greenwald I, Shaye DD (2018) OrthoList 2: A new comparative genomic analysis of human and *Caenorhabditis elegans* genes. *Genetics* 210(2):445–461
21. Hobert O, Specification of the nervous system (June 18, 2021), WormBook, ed. The *C. elegans* Research Community, WormBook, doi/<https://doi.org/10.1895/wormbook.1.7.1>, <http://www.wormbook.org>
22. Pinho-Ribeiro FA, Verri WA Jr, Chiu IM (2017) Nociceptor sensory neuron-immune interactions in pain and inflammation. *Trends Immunol* 38(1):5–19
23. Kahn-Kirby AH, Bargmann CI (2006) TRP channel in *C. elegans*. *Annu Rev Physiol* 68:719–736
24. Xiao R, Xu XS. *C. elegans* TRP Channels. In: Islam M. (eds) *Transient Receptor Potential Channels*. *Advances in Experimental Medicine and Biology*, 2011; 704:323–339. Springer, Dordrecht. https://doi.org/10.1007/978-94-007-0265-3_18
25. Glauser DA, Chen WC, Agin R, MacInnis B, Hellman AB, Garrity PA, Man-WahTan, Goodman MB (2011) Heat avoidance is regulated by Transient Receptor Potential (TRP) channels and a neuropeptide signaling pathway in *Caenorhabditis elegans*. *Genetics Society of America* 188:91–103
26. Venkatachalam K, Luo J, Montell C (2014) Evolutionarily conserved, multitasking TRP channels: lessons from worms and flies. *Handb Exp Pharmacol* 223:937–962
27. Nkambeu B, Ben Salem J, Leonelli S, Amin Marashi F (2019) Beaudry F (2019) EGL-3 and EGL-21 are required to trigger nociceptive response of *Caenorhabditis elegans* to noxious heat. *Neuropeptides* 73:41–48
28. Brenner S (1974) The genetics of *Caenorhabditis elegans*. *Genetics* 77:71–94
29. Margie O, Palmer C, Chin-Sang I (2013) *C. elegans* chemotaxis assay. *J Vis Exp* 74:1–6
30. Wittenburg N, Baumeister R (1999) Thermal avoidance in *Caenorhabditis elegans*: an approach to the study of nociception. *Proc Natl Acad Sci* 96(18):10477–10482
31. Zhou Y, Zhou B, Pache L, Chang M, Khodabakhshi AH, Tanaseichuk O, Benner C, Chanda SK (2019) Metascape provides a biologist-oriented resource for the analysis of systems-level datasets. *Nat Commun* 10:1523
32. Bindea G, Mlecnik B, Hackl H, Charoentong P, Tosolini M, Kirilovsky A, Fridman WH, Pagès F, Trajanoski Z, Galon J (2009) ClueGO: a Cytoscape plug-in to decipher functionally grouped gene ontology and pathway annotation networks. *Bioinformatics* 25(8):1091–1093
33. Shannon P, Markiel A, Ozier O, Baliga NS, Wang JT, Ramage D, Amin N, Schwikowski B, Ideker T (2003) Cytoscape: a software environment for integrated models of biomolecular interaction networks. *Genome Res* 13(11):2498–2504
34. Benjamini Y, Hochberg Y (1995) Controlling the false discovery rate: a practical and powerful approach to multiple testing. *J R Stat Soc Ser B* 57:289–300
35. Raisinghani M, Pabbidi RM, Premkumar LS (2005) Activation of transient receptor potential vanilloid 1 (TRPV1) by resiniferatoxin. *J Physiol* 567:771–786
36. Elokely K, Velisetty P, Delemotte L, Palovcak E, Klein ML, Rohacs T, Carnevale V. Understanding TRPV1 activation by ligands: Insights from the binding modes of capsaicin and resiniferatoxin. *Proceedings of the National Academy of Sciences* 2016;113: E137-145
37. Kim SR, Kim SU, Oh U, Jin BK (2006) Transient receptor potential vanilloid subtype 1 mediates microglial cell death in vivo and in vitro via Ca²⁺-mediated mitochondrial damage and cytochrome c release. *J Immunol*. Oct 1;177(7):4322–4329
38. Kun J, Helyes Z, Perkecz A, Bán Á, Polgár B, Szolcsányi J, Pintér E (2012) Effect of surgical and chemical sensory denervation on non-neural expression of the transient receptor potential vanilloid 1 (TRPV1) receptors in the rat. *J Mol Neurosci* 48(3):795–803
39. Tobin D, Madsen D, Kahn-Kirby A, Peckol E, Moulder G, Barstead R, Maricq A, Bargmann C (2002) Combinatorial expression of TRPV channel proteins defines their sensory functions and subcellular localization in *C. elegans* neurons. *Neuron* 35:307–318
40. Okerlund ND, Cheyette BNR (2011) Synaptic Wnt signaling—a contributor to major psychiatric disorders? *J Neurodev Disord* 3(2):162–174
41. Klassen MP, Shen K (2007) Wnt signaling positions neuromuscular connectivity by inhibiting synapse formation in *C. elegans*. *Cell* 130(4):24
42. Sani G, Napoletano F, Forte AM, Kotzalidis GD, Panaccione I, Porfiri GM, Simonetti A, Caloro M, Girardi N, Telesforo CL, Serra G, Romano S, Manfredi G, Savoia V, Tamorri SM,

- Koukopoulos AE, Serata D, Rapinesi C, Del Casale A, Nicoletti F, Girardi P (2010) The wnt pathway in mood disorders. *Curr Neuropharmacol* 10(3):239–253
43. Hussaini SM, Choi CI, Cho CH, Kim HJ, Jun H, Jang MH (2014) Wnt signaling in neuropsychiatric disorders: ties with adult hippocampal neurogenesis and behavior. *Neurosci Biobehav Rev* 47:369–383

Publisher's Note Springer Nature remains neutral with regard to jurisdictional claims in published maps and institutional affiliations.